

# Light scattering and viscosity studies of a ternary mixture with a double critical point

C. M. Sorensen and G. A. Larsen

*Department of Physics, Kansas State University, Manhattan, Kansas 66506*

(Received 15 March 1985; accepted 2 May 1985)

We have performed viscosity and dynamic light scattering measurements on the system 3-methylpyridine, water, and heavy water. This system displays a closed-loop coexistence curve which shrinks with increasing  $\text{H}_2\text{O}/\text{D}_2\text{O}$  ratio until the upper and lower consolute points merge at a double critical point. Our measurements were performed to study critical phenomena in this mixture in both the phase-separating and non-phase-separating regimes. We have found that the correlation length derived from our measurements diverges in both regimes with a power-law dependence on temperature relative to the double critical point temperature. The power-law exponent was double that usually found in ising-like liquid systems when the system was asymptotically far from the double critical point. Implications of this work for other non-phase-separating yet nonideal systems is discussed.

## I. INTRODUCTION

Binary fluid systems which unmix at a consolute temperature display critical phenomena near this point that is universal with other binary and liquid-gas systems.<sup>1</sup> These binary systems may be of the more common type which unmix below an upper critical solution temperature, UCST, or of the less common type which unmix upon heating above a lower critical solution temperature, LCST. In this paper we present both viscosity and light scattering measurements to study critical phenomena in a ternary system which has a closed-loop miscibility curve with both an UCST and a LCST. By varying the concentration of this mixture, the UCST and LCST could be caused to merge to a double critical point and subsequently disappear.

The phase behavior of fluid systems can be understood in terms of competition between energy and entropy factors. At high temperatures entropy is dominant and the fluids mix. As the temperature is lowered the entropy becomes less important and the system may unmix to two phases if like molecule interactions are energetically more favorable than unlike molecule interactions.<sup>2</sup> Some systems, most notable of which are aqueous hydrogen bonding systems, may have energetically favorable, but entropically unfavorable, unlike molecule directional interactions. This can cause, with the proper balance of parameters, a remixing of the components at still lower temperatures where the disfavorable directional interaction entropy loss effects are smaller than the favorable energy factor. Such a system is termed reentrant and displays a closed loop phase diagram on a composition-temperature graph. At the top and bottom of the loop are the UCST and LCST, respectively.

A number of theoretical studies have been presented to explain the phase diagrams of these systems over the last decade. Wheeler and Anderson<sup>3,4</sup> have used a decorated lattice gas model to describe the closed-loop phase diagram. More recently Walker, Vause, and Goldstein<sup>5</sup> have studied these systems with a position-space renormalization group method. All these methods involve some manner to allow a certain subset of molecular orientations to be energetically

more favorable than others, thus simulated the directional hydrogen bond and allowing for reentrance of the phases.

Our interest in these systems has been stimulated in two ways. First, the theoretical work has illustrated the fact that by varying, in some manner, the delicate balance between like and unlike molecule interactions the immiscibility loop can be made to shrink and disappear. As the UCST and LCST merge, a double critical point (DCP) is achieved. Near this DCP many of the critical-point exponents should approach values double that of their normal, single critical point values. Second, after the loop's disappearance, critical fluctuations may still occur in the homogeneous mixture near the former DCP. We wished to study such a "virtual" critical point because of its possible occurrence in other aqueous systems such as aqueous alcohol solutions or supercooled water.

In this paper we report viscosity and light scattering measurements on the quasibinary system, 3-methylpyridine (3MP), water, and heavy water. This system displays a closed-loop curve when the water concentration is zero, but the curve shrinks as the water content is increased until it disappears at a DCP. The 3MP/water system is totally miscible.

We have reported our results for the viscosity measurements previously<sup>6</sup> in a work we shall hereafter refer to as I. In that work we demonstrated that the exponent describing the viscosity's power-law divergence with relative temperature near a critical point nearly doubled as the loop closed. In the non-phase-separating systems the viscosity failed to diverge completely but showed a power-law divergence with doubled exponent when far away from the DCP temperature. In this work we include dynamic light scattering or photon correlation spectroscopy measurements of the correlation length for eight of the solutions studied in I. We found that the exponent for the correlation length doubled, that the viscosity exponent doubling was, as expected, just a reflection of the correlation length exponent doubling, and that the doubling can be explained in terms of the geometric picture of phase transitions described by Griffiths and Wheeler.<sup>7</sup>

Perhaps the earliest experimental work showing exponent doubling is that of Tufeu, Keyes, and Daniels<sup>8</sup> who measured correlation lengths and Rayleigh linewidths in a mixture of neon and krypton to show that the correlation length exponent  $\nu$  doubled for an isothermal approach with pressure towards a DCP. Deerenberg *et al.*<sup>9</sup> studied a similar gas-gas system, neon and xenon, and found the coexistence curve exponent  $\beta$  doubled near the DCP. Kortan *et al.*<sup>10</sup> studied reentrant behavior in a binary liquid crystal system to find the correlation length exponent doubled. Recently Johnston *et al.*<sup>11</sup> studied the quasibinary, closed-loop reentrant system guaiacol-glycerol-water with light scattering and again saw doubling near the DCP of the correlation length exponent.

The unifying picture for all this work is the geometric interpretation of Griffiths and Wheeler<sup>7</sup> to handle various paths of approach to a critical point. According to these authors, if the distance from the critical point is measured in terms of an intensive field variable, all paths of approach to the critical point are equivalent and use the same exponent except those that are tangent to the coexistence curve. Because the line of critical points experiences an extremum at a DCP, such a tangential path is possible near a DCP. Since the curvature of the critical line is, to first order, quadratic, the exponents along a tangential path are doubled.

We have studied ten solutions of different concentrations of 3MP and water and heavy water; five solutions which phase separate and five which do not. In Sec. II we describe our experimental procedure and in Sec. III our data analysis methods. We present our results in Sec. IV where we show that exponent doubling occurs when the system is far from the DCP compared to the size of the miscibility loop. Furthermore, the viscosity anomaly is a direct reflection of the correlation length anomaly. Section V contains our conclusions and speculations on anomalous behavior in various other aqueous systems which do not display a phase change.

## II. EXPERIMENT

The solutions of 3MP, H<sub>2</sub>O, and D<sub>2</sub>O were the same ones used in paper I. The 3MP was distilled over CaH<sub>2</sub> and collected over molecular sieves. The H<sub>2</sub>O was doubly distilled and the D<sub>2</sub>O was obtained from Aldrich Chemical Company and had an isotropic purity of 99.8%.

Cox's earlier study<sup>12</sup> for the phase separation behavior of this mixture indicated that the D<sub>2</sub>O/3MP (no H<sub>2</sub>O) system exhibited a closed loop with upper and lower critical solution points at 117 °C and 34% by weight 3MP and 38.5 °C and 28% by weight 3MP, respectively. He also gave data for a solution of 30% by weight 3MP in which the H<sub>2</sub>O/D<sub>2</sub>O ratio was varied to cause the eventual disappearance of the miscibility loop at 78 °C. Because of this and the ease of mixing solutions, we choose to study solutions which all had the same concentration of 3MP which for us turned out to be 29.9% by weight, near the average of the two critical concentrations. Two solutions, solutions 5 and 6, were adjusted in 3MP concentration in an attempt to get closer to the DCP. One might argue that it would be better to seek out the exact critical concentration at each H<sub>2</sub>O/D<sub>2</sub>O concentration, however, we shall see that the exponent doubling effects of

the double critical point are more apparent asymptotically far in temperature from the double critical temperature and hence small off-loading should not affect our results.

Two stock solutions 29.9% by weight of 3MP in either H<sub>2</sub>O or D<sub>2</sub>O were made. By mixing these solutions various ratios of H<sub>2</sub>O to D<sub>2</sub>O could be obtained while keeping the weight fraction of 3MP constant (although the mole fraction varied). Mixing and filling operations were performed volumetrically under dry nitrogen gas. Concentrations and phase separation temperatures of the ten solutions studied are given in Table I.

The viscosity measurement, described in I, used three different glass Poiseuille flow viscometers with volumes  $\sim 2$  cm and capillaries with diameters of 0.08 cm and length 15.0 cm. Temperature control was achieved by immersing a viscometer in a stirred water bath which was thermostated to  $\pm 0.01$  °C. Flow times were measured with a stopwatch. Densities of the solutions necessary to convert kinematic to shear viscosity were obtained gravimetrically from 20 to 80 °C using a 5 cm<sup>3</sup> pycnometer.

The viscosity  $\eta$  was found using

$$\eta = A \rho t \text{ (s)}, \quad (1)$$

where  $\rho$  is the density,  $t$  (s) the flow time in seconds, and  $A$  is a calibration constant which we determined by calibrating with water in the temperature range 20 to 85 °C. Our shear viscosity precision was better than  $\pm 1/2\%$ . Phase separation temperatures were determined visually to  $\pm 0.05$  °C.

The photon correlation light-scattering measurement was performed on eight of the solutions, solutions 6 and 9 were not used. The solutions were held in a 1 cm square spectrophotometer cuvette which was placed in a two-stage thermostated oven. This allowed for 1 mK control from 25 to 90 °C.

The light source was an argon ion laser operating at  $\lambda = 5145$  Å in the TEM<sub>00</sub> mode. This light was focused into the sample with a 30 cm focal length lens. Scattered light was collected with a 10 cm focal lens at 90° ( $\pm 1/2^\circ$ ). This lens focused a slightly demagnified image of the scattering volume onto a slit which could be adjusted to give good coherence on the cathode of an ITT FW130 photomultiplier tube 50 cm distant from the slit. The output of the photomultiplier was amplified and discriminated. These pulses were

TABLE I. Parameters for the ten solutions studied.  $T_{\text{sep}}$  = separation temperature if any, and  $\Delta T = 2|T_{\text{sep}} - 76^\circ\text{C}|$  = size of the miscibility loop.

Solution No.	Concentration (mol %)			$T_{\text{sep}}$ (°C)	$\Delta T$ (°C)
	3MP	D <sub>2</sub> O	H <sub>2</sub> O		
1	8.40	91.6	0	37.3	78.5
2	8.07	52.8	39.1	48.4	56.4
3	7.78	18.7	73.6	63.75	25.7
4	8.30	13.0	79.3	72.74, 80.20	7.46
5	8.30	12.9	78.8	74.9, 78.45	3.55
6	8.01	12.5	79.5	...	...
7	7.73	12.4	79.9	...	...
8	7.72	12.1	80.2	...	...
9	7.74	11.7	80.6	...	...
10	7.62	0	92.3	...	...

then fed to a commercial correlation which calculated the intensity autocorrelation function of the scattered light. The homodyne detection mode was used.

Analysis of the scattered light correlation function was performed with an on-line PDP 11/23 computer which performed a two cumulant fit to the data as shown in Eq. (2),

$$\langle I(0)I(t) \rangle = B + Ae^{-K_1 t + (1/2) K_2 t^2}. \quad (2)$$

Here  $K_1$  and  $K_2$  are the first two cumulants,  $A$  is the signal amplitude and  $B$  is the background.  $B$  was determined from the average of eight channels that were delayed 64 channels from the first 56 channels of the spectrum. In practice the background was varied manually slightly to obtain the best fit. The cumulant ratio  $K_2/K_1^2$ , which is a measure of the nonexponentiality of the spectrum, was usually less than 0.04 indicating the expected degree of exponentiality. Some solutions, however, when near ( $\sim 1^\circ\text{C}$ ) the phase separation temperatures gave larger degrees of nonexponentiality. This behavior correlated with the visual appearance of multiple scattering which will make the correlation function nonexponential.<sup>13</sup>

Our desire was to determine correlation lengths  $\xi$  of the solutions as a function of temperature. The most direct method of achieving such a measurement is to use the static light-scattering methods of turbidity or scattering anisotropy. The dynamic PCS measurement method we used had the disadvantage that it did not directly determine  $\xi$ , but required knowledge of the viscosity  $\eta$  as well. We, of course, had extensive viscosity measurements so this was not a problem for us. A further disadvantage is that far from the critical point background effects are important<sup>14,15</sup> and must be accounted for before reliable correlation lengths can be determined. Here again, as we will show below in our analysis, viscosity measurements can be used to develop a consistent method for the determination of the correlation length. The advantage of the dynamic technique is that it allows for measurement of small correlation lengths of the order of 10 to 20 Å which are difficult to determine using the static methods.

The correlation lengths we wished to study were those due to concentration fluctuations. Entropy fluctuations were also present and may have scattered light comparable in intensity to the concentration fluctuations far from the phase separation critical points. Entropy fluctuations are related to the thermal diffusivity<sup>16</sup> which may be estimated for our system to show that the correlation time  $\tau_c$  due to the entropy fluctuations,  $\tau_c = K_I^{-1}$ , is three orders of magnitude or more faster than those we measured, indicating that entropy fluctuations did not affect our measurements.

### III. DATA ANALYSIS

#### A. Viscosity

Near a critical point the viscosity is expected to behave the equation<sup>17</sup>

$$\eta = \eta_0(Q_0\xi)^\phi \quad (3a)$$

$$= \eta_0(Q_0\xi_0)^\phi t^{-x_\eta}. \quad (3b)$$

In Eq. (3a),  $\eta_0$  is the background viscosity which would be present if no critical anomaly occurred,  $Q_0$  is a wave number

dependent on the system, and  $\phi$  is a critical exponent. Equation (3b) uses the fact that  $\xi = \xi_0 t^{-\nu}$  where  $t$  is now, and hereafter, the reduced temperature,  $t = |T - T_c|/T_c$  where  $T_c$  is the critical temperature,  $\nu$  is the critical exponent for the correlation length, and  $x_\eta = \nu\phi$ . In I we used form (3b) for our analysis, here we shall rely more on Eq. (3a).

Our first task was to determine  $\eta_0$ . This may be accomplished by examining the behavior of the viscosity far from the critical point and then extrapolating this behavior into the critical region. This is always a problem because it is hard to determine where the anomaly effectively stops. Because of the systematic nature of our solutions with concentration, we were able to notice that far from their separation temperature the viscosities of the solutions were constant multiples of each other. To use this fact, we first fitted the viscosity of the solution with no D<sub>2</sub>O, which had the weakest anomaly, to a modified Arrhenius equation,  $\eta = \eta_0 \exp[-A/(T - T_0)]$ . By starting at  $10^\circ\text{C}$  and fitting to progressively more data, good fits were obtained until  $T > 35^\circ\text{C}$  when chi squared began to increase. This indicated the singular part of the viscosity was significant in these large  $T$  data. This fit gave us a background viscosity, which we call  $\eta_B$ , for this solution. It also gave a singular part which was symmetric about  $\sim 76^\circ\text{C}$  for this solution which could be inferred as necessary from the symmetric behavior of the other solutions as seen in Fig. 1. Figure 1 shows that the nonsingular parts of our data showed a linear correlation with D<sub>2</sub>O concentration. In fact this correlation had slope that was roughly equal to the viscosity difference between pure H<sub>2</sub>O and D<sub>2</sub>O at  $25^\circ\text{C}$ . Hence  $\eta_0$  for each solution was determined from the fit multiplied by the appropriate scaling factor determined from Fig. 1.

Solutions 1 and 2 do not appear to work well with this scheme. In Fig. 1 one can see that their low temperature behavior is considerably different than the other solutions.

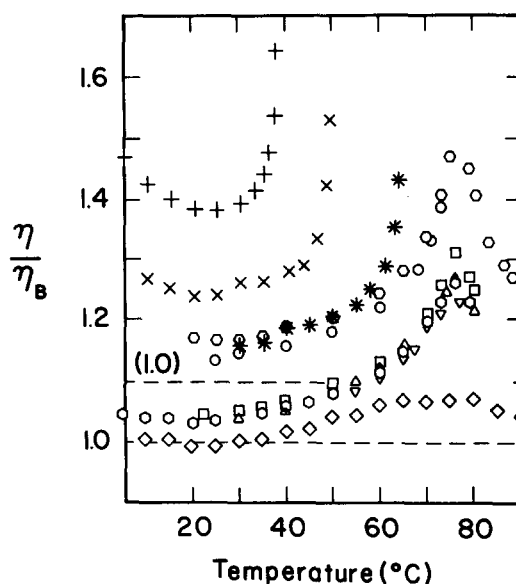


FIG. 1. Behavior of the viscosity with temperature relative to the background viscosity of solution 10,  $\eta_B$ . Symbols and solution numbers are: +, solution 1; x, solution 2; \*, solution 3; O, solution 4; □, solution 5; ◇, solution 6; △, solution 7; ▽, solution 8; ◇, solution 9; ◇, solution 10.

This is not surprising because their  $D_2O$  concentrations are considerably different. We have redetermined their background viscosities by fitting the data far from the separation temperature to the modified Arrhenius equation keeping  $T_0 = 150$  K. Similar fits to solutions 3 and 4 yielded only small changes compared to the method described above and hence were not used. Reanalysis of solutions 1 and 2 using these new backgrounds and Eq. (3b), i.e., the same analysis used in I, still yielded good fits, but with exponents of  $x_\eta = 0.042$  and  $0.051$ , rather than  $0.038$  and  $0.050$ , respectively, as reported in I.

## B. Light scattering

The light scattering data were analyzed by relating the measured first cumulant of the scattered light correlation function, Eq. (2), to the mutual diffusion coefficient  $D$  of the 3MP and "water" system using<sup>18</sup>

$$K_1 = 2Dq^2, \quad (4)$$

where  $q$  is the scattering wave number given by

$$q = \frac{4\pi n}{\lambda} \sin \theta / 2. \quad (5)$$

Here  $n$  is the refractive index of the solution and  $\theta$  is the scattering angle.

The refractive index for a 29.9% by weight 3MP in  $H_2O$  solution was found in the International Critical Tables<sup>19</sup> to be  $n = 1.39$  at  $25^\circ C$  and to vary slowly with 3MP concentration. Since the refractive indices for pure  $H_2O$  and  $D_2O$  at  $20^\circ C$  are  $1.3330$  and  $1.3384$ , respectively, we have assumed that addition of  $D_2O$  to the 3MP/ $H_2O$  solution does not change the refractive index by more than  $0.5\%$ . Temperature effects were estimated from the refractive index behavior with temperature of other liquids, including  $H_2O$ , to be  $0.02\%/^\circ C$ . Hence for all solutions we used  $n = 1.39 - 2 \times 10^{-4} [T(^\circ C) - 25]$ , which we estimate to be good to  $0.5\%$ .

Inversion of Eq. (4) yields the diffusion coefficient  $D$  which will have both a background and a critical part,

$$D = D_B + D_C. \quad (6)$$

Current results indicate that the critical part<sup>20</sup> is well described by

$$D_C = \frac{Rk_B T}{6\pi\eta\xi} \Omega_K(q\xi), \quad (7)$$

where  $k_B$  is Boltzmann's constant and  $R$  is a factor close to unity. We shall take  $R = 1.0$ . The Kawasaki function  $\Omega_K(q\xi)$  is given by<sup>21</sup>

$$\Omega_K(x) = \frac{3}{4x^2} [1 + x^2 + (x^3 - x^{-1}) \arctan x]. \quad (8)$$

The background part is given by<sup>22,23</sup>

$$D_B = \frac{k_B T}{16\eta_0\xi} \left[ \frac{1 + q^2\xi^2}{q_c\xi} \right]. \quad (9)$$

The wave number  $q_c$  is related to the viscosity wave number  $Q_0$  via

$$q_c = u Q_0. \quad (10)$$

To use Eqs. (6)–(9) the viscosity needs to be known

everywhere light scattering data are known. This is true for nearly all our data except for nine points above  $80^\circ C$ ; six points for solution 4 and three points for solution 7. The unknown viscosities for solution 4 were inferred from the viscosity of solution 5 which was uniformly slightly larger for  $T < 80^\circ C$ . The unknown viscosities for solution 7 were inferred from the symmetric behavior about  $76^\circ C$  seen in Fig. 1. Finally, solutions 1, 3, and 5 showed small differences in phase separation temperatures determined during the light scattering measurements when compared to those from the viscosity runs. In these cases the viscosities used were those with the same relative temperature,  $T - T_{sep}$ . This introduced an ambiguity of  $2\%$  or less.

Given a sequence of data involving temperature, first cumulant, and viscosity, it is possible to determine the correlation length  $\xi$ . To do this one must determine the magnitude of the background term, Eq. (9), hence one must know  $q_c$ . To determine  $q_c$ , however, one must know  $Q_0$  which in turn requires a knowledge of  $\eta/\eta_0$  and the constant  $u$ . The circular nature of this situation led us to the iterative scheme described below.

To start, for a given solution we assumed  $D_B = 0$  and numerically solved Eqs. (4), (7), and (8) for  $\xi$ . This first value of  $\xi$  was called  $\xi_1$ . Using  $\xi_1$ , we fitted  $\eta/\eta_0$  to Eq. (3a) to yield values for  $\phi$  and  $Q_0$ . Next  $q_c$  was calculated from  $Q_0$  using Eq. (10) and  $u = 4.0$ . This value of  $u$  has been suggested by Burstyn *et al.*<sup>24</sup> as the most realistic. Once  $q_c$  was determined we numerically solved the full expression, Eqs. (4)–(9), for  $\xi$ . This second iteration yielded  $\xi_2$ . The process was then repeated by fitting to Eq. (3a) to yield another  $Q_0$  and hence  $q_c$  and so forth. Fortunately, this iterative procedure converged rapidly at  $\xi_3$ , which had sufficient accuracy to be considered the true correlation length.

A flaw in this analysis was the imprecise knowledge of the constant  $u$  in Eq. (10). Small  $u$  yields small  $q_c$  which yields a large background component. We took the smallest value to be  $u = 1.5$  since it has been shown theoretically<sup>23</sup> that  $u \geq 1.9$ , but Burstyn and Sengers used  $1.5$  in one of their earlier analyses.<sup>25</sup> We performed our iterative analysis for using  $u = 1.5$  to give correlation lengths under the condition that the background was as large as reasonably possible. We also used  $u = 4.0$  which, according to Burstyn *et al.*,<sup>24</sup> should yield the most reasonable values of  $\xi$ , and  $u \rightarrow \infty$ , the first iteration, which represents  $\xi$  when there is no background contribution. Our results indicated that  $\xi$  changed tens of percent from one extreme to the other, but the power law with temperature dependence was affected much less. We shall comment on these effects in our discussion later.

By assuming a precisely known value for  $u$ , we have estimated the random error in  $\xi$ . Our experimental first cumulants were determined to  $\pm 2\%$ , viscosity to  $\pm 1/2\%$ ,  $q$  to  $\pm 1\%$ , and from the convergence behavior of our iterative scheme we estimate  $q_c$  is known to  $\pm 10\%$ . These errors led to a  $\pm 3\%$  uncertainty in  $\xi$  which increased to  $\pm 8\%$  at large  $\xi$ .

## IV. RESULTS

In I we showed how the viscosity of the phase separating solutions showed power-law behavior as  $T \rightarrow T_c$  with critical

exponents which nearly doubled from the normal value of  $x_\eta \simeq 0.04$  as the solutions approached the double critical point concentration. This behavior was somewhat dependent on the value of  $T_c$  chosen for the solutions which were adjusted slightly from the phase separation temperatures to yield the most linear behavior on a double logarithmic graph of  $\eta/\eta_0$  vs  $t = |T - T|/T_c$ . Perhaps a better way to demonstrate the exponent doubling is to graph  $\eta/\eta_0$  as a function of  $t_D = |T - T_D|/T_D^{-1}$ , the reduced temperature relative to the double critical point temperature  $T_D = 76.0^\circ\text{C}$ . Such a graph is given in Fig. 2 which includes the new values of  $\eta/\eta_0$  for solutions 1 and 2 derived from the new analysis of the background for these solutions.  $T_D$  was determined from the symmetry of both the  $\eta/\eta_0$  and correlation length data to be  $76.0 \pm 0.2^\circ\text{C}$ . Figure 2 shows that all the data for both separating and nonseparating solutions asymptotically approach a doubled exponent as  $t_D$  becomes large. Nonseparating solutions curve off as  $t_D \rightarrow 0$  because the double critical point is never actually reached, whereas the separating solutions diverge before  $t_D = 0$  because phase separation and an effective normal critical point intervene before the DCP can be reached. Identical behavior is seen in the correlation length and will be discussed in more detail below.

In Fig. 3 we graph  $\eta/\eta_0$  as a function of  $\xi$ . Slopes, corresponding to the exponent  $\phi$ , Eq. (3a), and values of  $Q_0$  for these graphs are given in Table II. Error estimates for  $Q_0$  were made by comparing graphs for  $u = 4.0$  and  $1.5$ . All eight solutions analyzed in this way show similar exponents with average value  $= 0.067$ . Theoretical predictions for the exponent include  $0.054$  and  $0.070$  from mode coupling theories<sup>26</sup> and  $0.065$  from the renormalization group.<sup>27</sup> Experimental results have ranged from  $0.046$  to  $0.068$ .<sup>28</sup> Values for solutions 1 and 2 are somewhat large. This may be due to an error in the background analysis. Our results are consistent

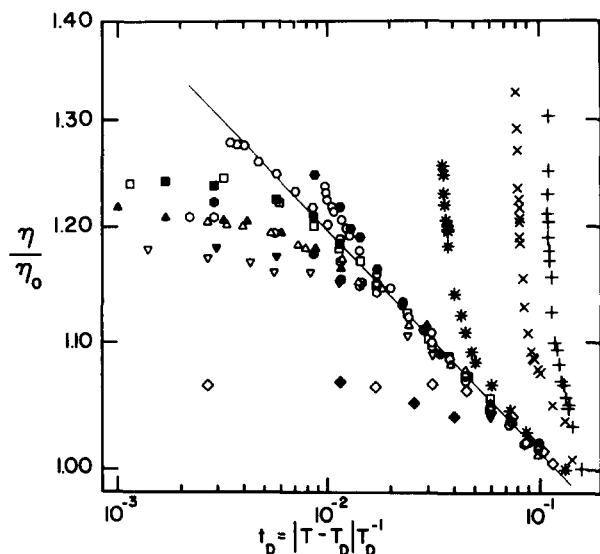


FIG. 2. Viscosity anomaly,  $\eta/\eta_0$ , as a function of the reduced temperature different,  $t_D$ , relative to the double critical point temperature,  $T_D = 76.0^\circ\text{C}$ . The thin line represents a limiting slope at large  $t_D$  of  $0.073$ . Symbols and solution numbers are: +, solution 1; ×, solution 2; \*, solution 3; ○, solution 4; □, solution 5; ◇, solution 6; △, solution 7; ▽, solution 8; ◇, solution 9; ◇, solution 10. Closed symbols are for  $T > T_D$ .

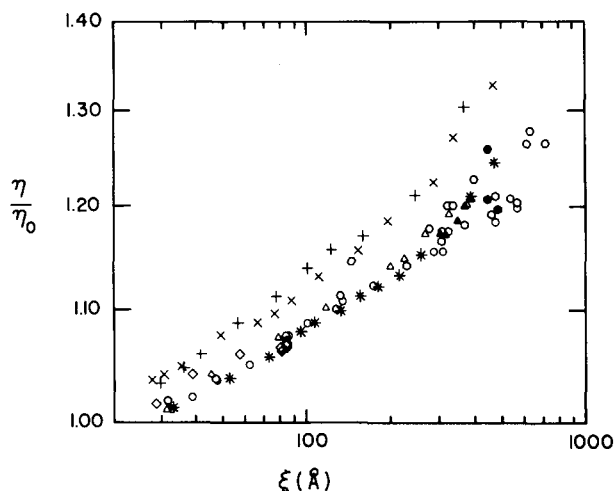


FIG. 4. The correlation length as a function of the temperature. Symbols and solution numbers are: +, solution 1; ×, solution 2; \*, solution 3; ○, solution 4; □, solution 5; ◇, solution 6; △, solution 7; ▽, solution 8; ◇, solution 9; ◇, solution 10. Closed symbols are for  $T > T_D$ .

with the expectations near a *single* critical point. This is reasonable because, as we shall see below, it is the correlation length exponent  $\nu$ , which is doubling near the DCP, which causes the exponent  $x_\eta = \nu\phi$  [Eq. (3b)] to double as  $\phi$  remains constant.

The second point to be made from Fig. 3 and Table II concerns the wave number  $Q_0$  which appears to have a small dependence on the  $\text{D}_2\text{O}/\text{H}_2\text{O}$  concentration. For solutions 3, 4, 5, 7, and 8, for which the  $\text{D}_2\text{O}/\text{H}_2\text{O}$  concentration is fairly much the same, the constancy of  $Q_0$  reinforces our opinion that our iterative analysis is at least consistent. Furthermore, comparison of Fig. 2 to Fig. 3 shows how the apparent broad range of behavior with temperature displayed in Fig. 2 reduces to a simple universal dependence on  $\xi$  as required by Eq. (3a). The behavior of  $\eta/\eta_0$  is just a mirror for the correlation length  $\xi$ .

To discuss the behavior of the correlation length, we begin with Fig. 4 which displays the results for all eight solutions studied with the light scattering as a function of temperature. The symmetry about  $76^\circ\text{C}$  is apparent. We also observe critical behavior in non-phase-separating solutions.

In Fig. 5 we have plotted  $\xi$  as a function of  $t_D = |T - T_D|/T_D^{-1}$  with  $T_D = 76.0 \pm 0.2^\circ\text{C}$ . The curves

TABLE II. Critical exponent  $\phi$  and wave number  $Q_0$  for the viscosity anomaly  $\eta/\eta_0 = (Q_0\xi)^\phi$ . The estimated errors in  $\phi$  and  $Q_0$  are  $\pm 0.003$  and  $\pm 0.3 \times 10^{-2} \text{Å}^{-1}$ , respectively, except for solution 10 where the errors are estimated to be  $\pm 0.008$  and  $\pm 1.5 \times 10^{-2} \text{Å}^{-1}$ , respectively.

Solution No.	$\phi$	$Q_0(\text{Å}^{-1})$
1	0.077	$5.0 \times 10^{-2}$
2	0.073	$5.2 \times 10^{-2}$
3	0.066	$3.3 \times 10^{-2}$
4	0.062	$3.7 \times 10^{-2}$
5	0.073	$3.6 \times 10^{-2}$
7	0.064	$3.6 \times 10^{-2}$
8	0.067	$3.7 \times 10^{-2}$
10	0.055	$4.5 \times 10^{-2}$

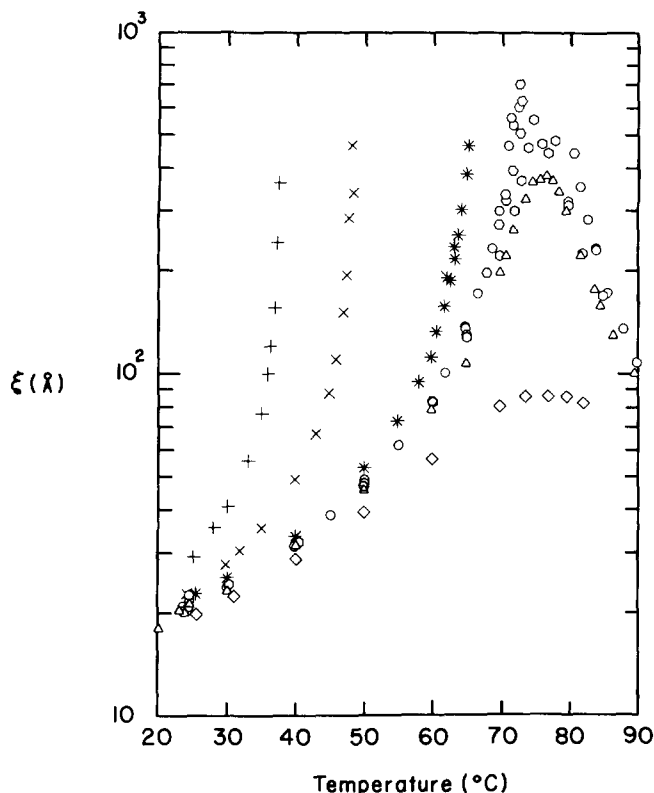


FIG. 4. The correlation length as a function of the temperature. Symbols and solution numbers are: +, solution 1; ×, solution 2; \*, solution 3; ○, solution 4; □, solution 5; ◇, solution 7; △, solution 8; ◇, solution 10. Closed symbols are for  $T > T_D$ .

are very similar to those for  $\eta/\eta_0$  in Fig. 2 as expected from Fig. 3 and our conclusions therewith. Exponent doubling of  $\nu$  to  $2\nu$  is seen at large  $t_D$  when the deviations of the solutions from the DCP are small compared to the deviation from the DCP represented by  $t_D$ . We shall elaborate more on this below.

The limiting slope at large  $t_D$  in Fig. 5 can be estimated to be  $1.22 \pm 0.03$  which is nearly double the current "best

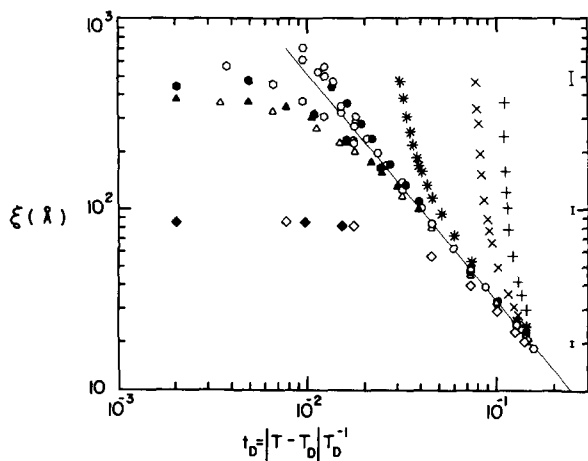


FIG. 5. Correlation length as a function of the reduced temperature difference,  $t_D$ , relative to the double critical point temperature,  $T_D = 76.0^\circ\text{C}$ . The thin line represents a limiting slope at large  $t_D$  of 1.22. Error bars are given on the right. Symbols and solutions are: +, solution 1; ×, solution 2; \*, solution 3; ○, solution 4; □, solution 5; ◇, solution 7; △, solution 8; ◇, solution 10. Closed symbols are for  $T > T_D$ .

value" for the critical exponent,  $\nu = 0.63$ . We have created similar graphs for the case of no background contribution to the diffusion coefficient, which corresponds to  $u \rightarrow \infty$  in Eq. (10), and the largest reasonable background contribution using  $u = 1.5$ . These graphs showed the same qualitative behavior but with limiting slopes of 1.33 and 1.04, respectively. Thus it appears the value of  $u = 4$  is not only bracketed by these two extremes but yields exponent doubling most closely.

To analyze these results further we shall fit our data to theoretical forms given by Kortan *et al.*<sup>10</sup> and Johnston *et al.*<sup>11</sup> Both groups have proposed nearly the same functional forms for the correlation length in a system with a double critical point. We shall use the analysis of Johnston *et al.* because they showed how it follows from the Griffiths and Wheeler geometric picture of critical points.

Johnston *et al.* assumed that the line of critical points is a function of the concentration  $x$  given by

$$(T_U - T_L)/T_D \equiv \Delta t = 2A(x - x_D)^{1/2} \quad (11)$$

and

$$(T_U + T_L)/2T_D = 1 + C(x - x_D). \quad (12)$$

Here  $T_U$  and  $T_L$  are the upper and lower critical temperatures,  $x_D$  is the double critical point concentration, where in our case  $x$  is the  $\text{D}_2\text{O}$  concentration, and  $A$  and  $C$  are constants.

In our analysis we assumed that the asymmetric term in Eq. (12) was zero, i.e.,  $C = 0$ . We have done this for a variety of reasons. First, we have determined  $T_U$  for only two systems, hence an accurate fit could not be made. We fit Cox's data<sup>12</sup> to Eq. (12) and found a small but finite  $C$ , but while our values for  $T_L$  agreed well with Cox's for large  $x - x_D$ , larger deviations developed as  $x \rightarrow x_D$ . Thus, we were uncertain of the applicability of Cox's value to our data. In fact any fit of our separation temperatures to Eqs. (11) and (12) must result in some uncertainty because we were not precisely on the critical isochore. Hence the extra precision given by Eq. (12) seemed unwarranted. A fit to Eq. (11), on the other hand, must be performed despite these uncertainties because it is the parabolic nature of Eq. (11) as well as the coefficient  $A$  that determine the exponent doubling and asymptotic regime of doubling.

To fit our data to Eq. (11) we assumed that the separation temperatures could be used as critical temperatures  $T_U$  and  $T_L$ , which is probably accurate to  $1^\circ\text{C}$ , and that  $T_U = T_L + 2(T_D - T_L)$  when  $T_U$  was not known. We also let the exponent on  $(x - x_D)$  vary. We found the data were well described by  $\Delta t = 2A(x - x_D)^{1/a}$ , where  $A = 0.127 \pm 0.03$  and  $a = 2.1 \pm 0.1$ .

Following Johnston *et al.*,<sup>11</sup> the concentration dependence of the correlation length as a critical point is approached should be of the form  $|x_C(T) - x|^{-\nu}$  where  $x_C$  is the temperature dependent critical concentration. Setting  $x = x_C$ ,  $C = 0$ , and eliminating  $T_U$  from Eqs. (11) and (12) one finds

$$x_C - x_D = \frac{1}{A^2} t_D^2. \quad (13)$$

It then follows that for  $x > x_D$ , i.e., phase-separating solutions

$$\xi = \xi_0 [t_D^2 - \frac{1}{4} \Delta t^2]^{-\nu} \quad (14)$$

and for  $x < x_D$ , i.e., non-phase-separating solutions

$$\xi = \xi_0 [t_D^2 + A^2(x_D - x)]^{-\nu}. \quad (15)$$

These are identical to the results of Johnston *et al.* in the limit  $C \rightarrow 0$ .

We graphically compared our data to Eqs. (14) and (15) by plotting  $\xi^{-1/\nu}$  vs  $t_D^2$  with  $\nu = 0.63$ . The slope of such graphs should be equal to  $\xi_0^{-1/\nu}$  and the intercepts should be related to  $(x_D - x)$ . Figures 6 and 7 display our data plotted in such a manner. Figure 7 is a higher resolution version of Fig. 6 at small  $t_D$ . The linearity of these graphs testifies to the accuracy of Eqs. (14) and (15).

Table III lists the values of  $\xi_0$  for the eight solutions studied by light scattering. The values of  $\xi_0$  for solutions 3, 4, 5, 7, 8, and 10 are all very consistent with each other. The anomaly in solution 10 is small so the errors are larger. Solutions 1 and 2 have slightly smaller  $\xi_0$  values but also have significantly different  $D_2O$  concentrations. These results suggest that  $\xi_0$  has a small dependence on  $D_2O$  concentration.

Also listed in Table III are the measured intercepts compared to those calculated using  $A^2(x - x_D) \xi_0^{-1/\nu}$ . Good agreement is seen for the larger intercepts. Agreement is not as good for smaller intercepts where the relative error is larger. However, all the calculated intercepts are systematically

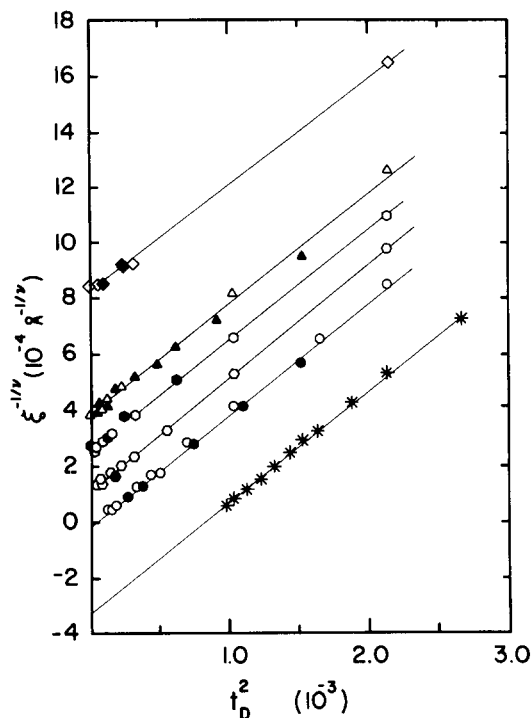


FIG. 7. Correlation length in angstroms raised to the  $-\nu^{-1}$  power vs the square of the reduced temperature,  $t_D^2$ . This is a high resolution version of Fig. 6. Straight line behavior is expected from Eqs. (14) and (15) of the text. As in Fig. 6 some of the plots have been shifted upward for clarity. Symbols, solution numbers, and upward shifts are: \*, solution 3, no shift;  $\circ$ , solution 4, no shift;  $\circ$ , solution 5,  $1 \times 10^{-4}$ ;  $\circ$ , solution 7,  $2 \times 10^{-4}$ ;  $\triangle$ , solution 8,  $3 \times 10^{-4}$ ;  $\diamond$ , solution 10, no shift. Closed symbols are for  $T > 76^\circ\text{C}$ .

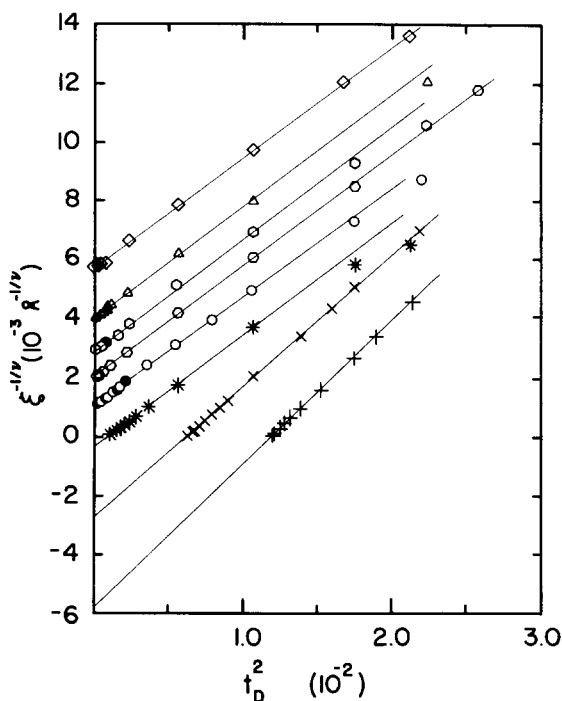


FIG. 6. Correlation length in angstroms raised to the  $-\nu^{-1}$  power vs the square of the reduced temperature,  $t_D^2$ . Straight line behavior is expected from Eqs. (14) and (15) of the text. For clarity some of the plots have been shifted upwards by various amounts. Symbols, solution numbers, and upward shifts are: +, solution 1, no shift;  $\times$ , solution 2, no shift; \*, solution 3, no shift;  $\circ$ , solution 4,  $1 \times 10^{-3}$ ;  $\circ$ , solution 5,  $2 \times 10^{-3}$ ;  $\circ$ , solution 7,  $3 \times 10^{-3}$ ;  $\triangle$ , solution 8,  $4 \times 10^{-3}$ ;  $\diamond$ , solution 10,  $5 \times 10^{-3}$ . Closed symbols are for  $T > 76^\circ\text{C}$ .

$\sim 3 \times 10^{-5}$  smaller than the measured intercepts. We have no explanation for this small difference. In summary, however, Eqs. (14) and (15) describe the data very well.

## V. CONCLUSIONS

We have shown that critical exponent doubling for both the viscosity and correlation length occurs near the double critical point of the quasibinary mixture 3-methylpyridine, water, and heavy water. The source of the doubling could be explained in terms of an approach parallel to the critical line of this mixture using the geometric picture of critical phenomena presented by Griffiths and Wheeler. Such an approach to the DCP of a quadratic critical curve should, as shown by Johnston *et al.*, yield doubled exponents. Instead of examining the anomalies relative to the upper and lower

TABLE III. Values of  $\xi_0$  and intercepts determined from slope-intercept fits to Eqs. (14) and (15) in Figs. 6 and 7.

Solution No.	$\xi_0(A)$	Measured intercept	Calculated intercept
1	1.57	$-5.8 \times 10^{-3}$	$-5.85 \times 10^{-3}$
2	1.66	$-2.75 \times 10^{-3}$	$-2.78 \times 10^{-3}$
3	1.79	$-3.3 \times 10^{-4}$	$-3.7 \times 10^{-4}$
4	1.79	$-2 \times 10^{-5}$	$-5 \times 10^{-5}$
5	1.76	0	$-3 \times 10^{-5}$
7	1.78	$6 \times 10^{-5}$	$2 \times 10^{-5}$
8	1.79	$8 \times 10^{-5}$	$4 \times 10^{-5}$
10	1.82	$8.2 \times 10^{-4}$	$8.1 \times 10^{-4}$

critical solution temperatures, however, we have compared them all to the DCP temperatures, as shown in Figs. 2 and 5. These graphs display a family of curves which all asymptotically approach a power law with doubled exponent for large  $t_D = |T - T_D|T_D^{-1}$ . The asymptotic regime is for reduced temperatures  $t_D$  which are large compared to the reduced width of the loop for the phase-separating mixtures, or equivalently, the effective reduced width for non-phase-separating mixtures. Hence, one might state that the parallel nature of the approach to the critical curve is relative to the distance from the critical curve. Finally, we have seen that the anomaly in the viscosity is a direct reflection of the anomaly in the correlation length as expected from Eq. (3a).

While these results have, we hope, an intrinsic interest of their own, they also have possibly interesting implications for other systems. In particular, we find stimulation in the appearance of critical phenomena in the non-phase-separating mixtures. Is it possible that other aqueous systems display various degrees of critical phenomena without actually phase separating?

It is well known that numerous aqueous solutions are quite nonideal and have a variety of unusual properties.<sup>29</sup> These properties are often explained in terms of hydrophobic and hydrophilic interactions between the water and its solute. Strong, and often delicately balanced, enthalpic and entropic effects occur. These like and unlike interactions and energy-entropy competitions were the ingredients used at the beginning of this paper to describe phase separation behavior. It is standard procedure to use the nonideality of a solution to explain phase separation and critical points, but perhaps it would be worthwhile to argue the converse: use proximity to critical points, even if they are not on the phase diagram, to explain certain properties of nonideal solutions.

An obvious example is the system 3MP/H<sub>2</sub>O which does not phase separate but is very nonideal, and displays some critical opalescence. Its proximity to a hidden or virtual critical point not on its phase diagram can be used to explain these facts as well as to predict various anomalies in other transport or thermodynamic properties.

Perhaps more subtle would be to consider the notorious alcohol plus water systems with this picture.<sup>30</sup> Alcohols are mixed solutes having both hydrophilic and hydrophobic parts and the smaller miscible alcohols may unmix from water with application of pressure or addition of ionic salts.<sup>31</sup> The unusual thermodynamic properties of these systems might be effectively understood in terms of critical fluctuations due to a critical point in some other direction, e.g., pressure or salt concentrating, of the phase diagram.

Finally, we remark that pure supercooled water displays anomalies that are similar to those seen near a critical point.<sup>32</sup> Furthermore, these anomalies may be enhanced by addition of various mixed solutes.<sup>33,34</sup> Perhaps it would be fruitful to study supercooled aqueous solutions for phase

separation behavior which, while not present in the pure water system, have critical points which influence the behavior of supercooled water.

This work was supported by NSF Grant CHE82-19571.

- <sup>1</sup>J. V. Sengers and J. M. H. Levelt Sengers, in *Progress in Liquid Physics*, edited by C. A. Croxton (Wiley, New York, 1978), p. 103.
- <sup>2</sup>J. D. Hirschfelder, D. Stevenson, and H. Eyring, *J. Chem. Phys.* **5**, 896 (1937).
- <sup>3</sup>J. C. Wheeler, *J. Chem. Phys.* **62**, 433 (1975).
- <sup>4</sup>G. R. Anderson and J. C. Wheeler, *J. Chem. Phys.* **69**, 2082, 3403 (1978); **73**, 5778 (1980).
- <sup>5</sup>J. S. Walker and C. A. Vause, *Phys. Lett.* **79 A**, 421 (1980); **90**, 419 (1982); R. E. Goldstein and J. S. Walker, *J. Chem. Phys.* **78**, 1942 (1983); R. E. Goldstein, *ibid.* **79**, 4439 (1983).
- <sup>6</sup>G. A. Larsen and C. M. Sorensen, *Phys. Rev. Lett.* **54**, 343 (1985).
- <sup>7</sup>R. B. Griffiths and J. C. Wheeler, *Phys. Rev. A* **2**, 1047 (1970).
- <sup>8</sup>R. J. Tufeu, P. H. Keyes, and W. B. Daniels, *Phys. Rev. Lett.* **35**, 1004 (1975).
- <sup>9</sup>A. Deerenberg, J. A. Schouten, and N. J. Trappeniers, *Physica (Utrecht)* **103 A**, 183 (1980).
- <sup>10</sup>A. R. Kortan, H. V. Kanel, R. J. Birgeneau, and J. D. Litster, *Phys. Rev. Lett.* **47**, 1206 (1981).
- <sup>11</sup>R. G. Johnston, Ph.D. thesis, University of Colorado, 1983 (unpublished); G. Johnston, N. A. Clark, P. Wiltzius, and D. S. Cannell, *Phys. Rev. Lett.* **54**, 49 (1985).
- <sup>12</sup>J. D. Cox, *J. Chem. Soc. (London)* **1952**, 4606.
- <sup>13</sup>C. M. Sorensen, R. C. Mockler, and W. J. O'Sullivan, *Phys. Rev. A* **16**, 365 (1977).
- <sup>14</sup>H. L. Swinney and D. L. Henry, *Phys. Rev. A* **8**, 2586 (1973).
- <sup>15</sup>D. L. Henry, L. E. Evans, and R. Kobayashi, *J. Chem. Phys.* **66**, 1802 (1977).
- <sup>16</sup>R. D. Mountain, *Rev. Mod. Phys.* **38**, 205 (1966).
- <sup>17</sup>T. Ohta, *J. Phys. C* **10**, 791 (1977).
- <sup>18</sup>B. J. Berne and R. Pecora, *Dynamic Light Scattering* (Wiley, New York, 1976).
- <sup>19</sup>*International Critical Tables* (McGraw-Hill, New York, 1926), Vol. 3.
- <sup>20</sup>H. C. Burstyn and J. V. Sengers, *Phys. Rev. A* **25**, 488 (1982).
- <sup>21</sup>K. Kawasaki, in *Phase Transitions and Critical Phenomena*, edited by C. Domb and M. S. Green (Academic, New York, 1976), Vol. 5a, p. 165.
- <sup>22</sup>D. W. Oxtoby and W. M. Gelbart, *J. Chem. Phys.* **61**, 2957 (1974).
- <sup>23</sup>J. K. Bhattacharjee, R. A. Ferrell, R. S. Basu, and J. V. Sengers, *Phys. Rev. A* **24**, 1469 (1981).
- <sup>24</sup>H. C. Burstyn, J. V. Sengers, J. K. Bhattacharjee, and R. A. Ferrell, *Phys. Rev. A* **28**, 1567 (1983).
- <sup>25</sup>H. C. Burstyn and J. V. Sengers, in *Proceedings of the Eighth Symposium on Thermophysical Properties*, edited by J. V. Sengers (American Society of Mechanical Engineers, New York, 1982), Vol. 1.
- <sup>26</sup>F. Garisto and R. Kapral, *Phys. Rev. A* **14**, 884 (1976).
- <sup>27</sup>E. D. Siggia, B. I. Halperin, and P. C. Hohenberg, *Phys. Rev. B* **13**, 2110 (1976).
- <sup>28</sup>S. P. Lee, *Chem. Phys. Lett.* **57**, 611 (1978).
- <sup>29</sup>F. Franks, in *Water, A Comprehensive Treatise*, edited by F. Franks (Plenum, New York, 1973), Vol. 2.
- <sup>30</sup>F. Franks and D. J. G. Ives, *Q. Rev. (London)* **20**, 1 (1966).
- <sup>31</sup>G. Schneider, *Ber. Bunsenges, Phys. Chem.* **76**, 325 (1972).
- <sup>32</sup>C. A. Angell, in *Water, A Comprehensive Treatise*, edited by F. Franks (Plenum, New York, 1982), Vol. 7.
- <sup>33</sup>B. L. Halfpap and C. M. Sorensen, *J. Chem. Phys.* **77**, 466 (1982); G. W. Euliss and C. M. Sorensen, *ibid.* **80**, 4767 (1984).
- <sup>34</sup>R. J. Speedy, J. A. Ballance, and B. D. Cornish, *J. Phys. Chem.* **87**, 325 (1983).